

# Feedback Identification of conductance-based models <sup>★</sup>

Thiago B. Burghi <sup>a</sup>, Maarten Schoukens <sup>b</sup>, Rodolphe Sepulchre <sup>a</sup>

<sup>a</sup>*Department of Engineering, Control Group, University of Cambridge, Cambridge CB2 1PZ, UK.*

<sup>b</sup>*Department of Electrical Engineering, Eindhoven University of Technology, 5612 AZ Eindhoven, Netherlands.*

---

## Abstract

This paper applies the classical prediction error method (PEM) to the estimation of nonlinear models of neuronal systems subject to input-additive noise. While the nonlinear system exhibits excitability, bifurcations, and limit-cycle oscillations, we prove consistency of the parameter estimation procedure under output feedback. Hence, this paper provides a rigorous framework for the application of conventional nonlinear system identification methods to stochastic neuronal systems. The main result exploits the elementary property that conductance-based models of neurons have an exponentially contracting inverse dynamics. This property is implied by the voltage-clamp experiment, which has been the fundamental modeling experiment of neurons ever since the pioneering work of Hodgkin and Huxley.

*Key words:* Closed-loop identification, nonlinear system identification, prediction error methods, contraction theory, neuronal systems, output feedback.

---

## 1 Introduction

The estimation of models for biological neuronal systems is a topic that has attracted considerable interest in the scientific community over the past decades [29,11,17,21,28]. However, the asymptotic properties of published estimation methods are rarely discussed. This is understandable for models that exhibit highly nonlinear dynamics including excitable behaviors and limit cycle oscillations.

The goal of this paper is to show that rigorous convergence results can be established in the most classical framework of the prediction error method (PEM) [22,23]. In nonlinear system identification, the convergence and consistency analysis of the PEM is made tractable by two well-known assumptions: (i) the true system includes output-additive noise but no input-additive noise [32,24], and (ii) the signals are generated by a system with some form of input-output stability — for instance, a fading memory [2], input-output exponential stability [22,30], or mean-square convergence of the output to that of a Volterra series [31,32].

Neuronal systems fail to satisfy both of these two assumptions. First, neuronal systems are primarily subject to *input*-additive noise. This noise models the stochastic fluctuations of currents traversing the neuronal membrane. For a review of the modeling of noise in neuronal systems, see [13,12]. Furthermore, the non-equilibrium nature of neuronal behaviors excludes any reasonable exponential stability or fading memory assumption.

Previous works have studied the application of the PEM under these unfavorable conditions. Under an assumption of exponential stability, but allowing for process noise, [30] developed a framework to identify block-oriented (also called structured) nonlinear systems with known LTI elements. In [5], the authors justify with dynamical systems theory the application of the PEM to identify the linear element of a Lure-type system with a limit cycle; the authors have to make an ergodicity assumption in order to prove consistency of the parameters estimates. As an alternative to the PEM, [26] developed a method based on transverse contraction analysis to identify oscillatory systems under the assumption that all states of the model are available; no noise considerations are made.

The main observation underlying the present paper is that while the fundamental assumptions of the PEM are not verified for conductance-based neuronal models, they hold for their inverse. In other words, conductance-

---

<sup>★</sup> Corresponding author T. B. Burghi.

*Email addresses:* [tbb29@cam.ac.uk](mailto:tbb29@cam.ac.uk) (Thiago B. Burghi), [m.schoukens@tue.nl](mailto:m.schoukens@tue.nl) (Maarten Schoukens), [r.sepulchre@eng.cam.ac.uk](mailto:r.sepulchre@eng.cam.ac.uk) (Rodolphe Sepulchre).

based models satisfy the required assumptions of PEM under high-gain output feedback. This means that neuronal systems can be identified with classical techniques by relying on the direct approach of closed-loop system identification [10]. Using contraction theory [25], we rigorously justify the use of the direct approach to consistently estimate neuronal model parameters.

We show that the closed-loop approach to the neuronal system identification problem is fully consistent with the classical voltage-clamp experiment of Hodgkin and Huxley [15]. Voltage-clamp has remained to date the key experimental methodology to derive a state-space model of a neuron. We show that there is flexibility in designing a contracting output feedback law beyond the high-gain implementation of voltage-clamp. As in previous work dealing with Lure systems [3], we advocate that feedback design is an integral element of neuronal system identification, which makes this an attractive application of closed-loop system identification theory.

The paper is organized as follows: in Section 2, we review a number of classical tools of nonlinear system identification and analysis. In Section 3, we introduce the general class of conductance-based models and show that they have a contracting inverse. In Section 4, we detail the identification of the inverse dynamics of neuronal systems with the PEM and discuss the plausibility of the required assumptions. We then conclude with Section 6.

## 2 Preliminaries

This section reviews two classical results of system theory: the convergence properties of the prediction error method [22] and the system property of contraction [25].

We use the following notation: For a discrete-time variable  $x_k$ , the signal up to time  $k$  is denoted by  $x_{[0,k]} = (x_k, x_{k-1}, \dots, x_0)$ . We write  $\mathbb{R}_+ = [0, \infty)$  and  $\mathbb{Z}_+ = \{0, 1, \dots\}$ , and the number 0 is treated as a scalar or as a vector, with the dimension implied by the context in which it is used. The norms  $\|\cdot\|_p$  denote the usual  $p$  norms of the Euclidean spaces, and  $\sigma_{\max}[\cdot]$  denotes the largest singular value of a matrix. For arbitrary  $\beta > 0$ , the class of  $n_u$ -valued sequences  $u : \mathbb{Z}_+ \rightarrow \mathbb{R}^{n_u}$  such that  $\sup_{k \in \mathbb{Z}_+} \|u_k\|_\infty < \beta$  is denoted by  $\mathcal{U}_\beta^{n_u}$ . We will also use the notation  $\mathcal{U}_\beta^{n_u}$  to denote the set of  $n_u$ -valued functions  $u : \mathbb{R}_+ \rightarrow \mathbb{R}^{n_u}$  such that  $\sup_{t \in \mathbb{R}_+} \|u(t)\|_\infty < \beta$ . We rely on context to make clear when  $\mathcal{U}_\beta^{n_u}$  refers to a class of sequences or functions.

### 2.1 Parametric Identification of nonlinear systems with the Prediction Error Method

Consider a nonlinear stochastic discrete-time system represented by

$$y_k = F_k(u_{[0,k]}; x_0) + e_k \quad (1)$$

where  $u_k \in \mathbb{R}^{n_u}$  is the system's input,  $y_k \in \mathbb{R}^{n_y}$  is the system's output,  $e_k \in \mathbb{R}^{n_y}$  is a stochastic process such that  $E[e_k | e_{[0,k-1]}] = 0$ ,  $F_k(\cdot)$  is a sequence of deterministic mappings, and  $x_0$  is an initial state.

Assume that the system (1) is in a feedback loop with an adaptive feedback element given by

$$u_k = H_k(y_{[0,k-1]}, u_{[0,k-1]}, r_k) \quad (2)$$

where  $u_k$  is the feedback element's output,  $y_k$  is the output of (1), and  $r_k \in \mathbb{R}^{n_r}$  is an external signal. Figure 1 shows a block diagram representation of the resulting feedback system<sup>1</sup>.

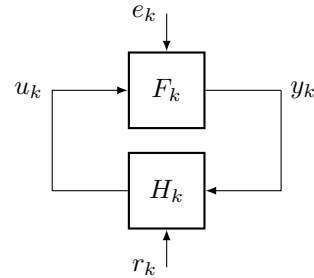


Fig. 1. Standard closed-loop identification setup.

In the prediction error framework, the system (1) is identified based on  $N$  collected input-output data points, given by the sequences  $y_{[0,N]}$  and  $u_{[0,N]}$ . For this purpose, a parametric model is used to obtain a prediction  $\hat{y}_k$  of the output  $y_k$ . In this paper, we work with an *output error* model, which is represented by a sequence of operators  $\hat{F}_k$  such that

$$\hat{y}_k(\theta) = \hat{F}_k(u_{[0,k]}; \theta) \quad (3)$$

where  $\theta \in \mathcal{D}$  denotes a vector of parameters, and  $\mathcal{D}$  is a subset of  $\mathbb{R}^{n_\theta}$ , with  $n_\theta$  the number of parameters.

A simple criterion that can be used to obtain estimates for the parameters in the vector  $\theta$  is the minimization of the cost function

$$V_N(\theta) = \frac{1}{N} \sum_{k=1}^N (y_k - \hat{y}_k(\theta))^2, \quad (4)$$

resulting in the parameter estimates

$$\hat{\theta}_N = \arg \min_{\theta \in \mathcal{D}} V_N(\theta) \quad (5)$$

<sup>1</sup> In (1) and (3), we allow the input to affect the output without a delay. This differs from the text in [22], where a time delay is assumed. However, as remarked in [22], this delay is not essential for their results. To make clear that algebraic loops are not allowed in the system, we included an explicit time delay in the subsystem (2).

The asymptotic behavior of the parameter estimates  $\hat{\theta}_N$  as the number of data points  $N$  grows to infinity depends on the asymptotic behavior of the function  $V_N(\theta)$ . Since the system is stochastic,  $V_N(\theta)$  is a random variable. To guarantee that the identified model is independent of the specific realization of the noise entering the system, we need the prediction error  $\varepsilon_k(\theta) = y_k - \hat{y}_k(\theta)$  to satisfy an ergodicity property:  $V_N(\theta)$  must converge to its expected value as  $N \rightarrow \infty$ . This property is achieved by means of two fundamental conditions: one on the true system, and one on the model structure.

**Condition 1** ([22],[10]). The closed-loop system (1)-(2) is such that for each  $k, s \in \mathbb{Z}_+, k \geq s$ , there exist random variables  $\bar{y}_{k,s}$  and  $\bar{u}_{k,s}$ , independent of  $r_{[0,s]}$  and  $e_{[0,s]}$  but not independent of  $r_{[0,k]}$  and  $e_{[0,k]}$ , such that

$$E [\|y_k - \bar{y}_{k,s}\|^4] < C\alpha^{k-s} \quad (6a)$$

$$E [\|u_k - \bar{u}_{k,s}\|^4] < C\alpha^{k-s} \quad (6b)$$

for some  $C > 0$  and  $\alpha < 1$ . Here,  $\bar{y}_{s,s} = \bar{u}_{s,s} = 0$ .

**Condition 2** ([22]). The mappings  $\hat{F}_k$  are differentiable with respect to  $\theta$  for all  $\theta \in \mathcal{D}$ , where  $\mathcal{D}$  is a closed and bounded subset of  $\mathbb{R}^{n_\theta}$ . Furthermore, there exist a  $C < \infty$  and  $\alpha < 1$  such that

$$\begin{aligned} & \|\hat{F}_k(u_{[0,k]}; \theta) - \hat{F}_k(\tilde{u}_{[0,k]}; \theta)\| \\ & \leq C \sum_{m=0}^k \alpha^{k-m} \|u_m - \tilde{u}_m\| \end{aligned} \quad (7)$$

and

$$\|\hat{F}_k(0_{[0,k]}; \theta)\| \leq C \quad (8)$$

for all  $k, u_{[0,k]}, \tilde{u}_{[0,k]}$ , and  $\theta$  belongs to an open neighborhood of  $\mathcal{D}$ . The  $(d/d\theta)\hat{F}_k$  are subject to an inequality analogous to (7).

When the model (3) satisfies Condition 2, then the mapping  $\theta \mapsto \{\hat{F}_k(\cdot; \theta)\}_{k \in \mathbb{Z}_+}$  is called a model structure [23, Section 5.7]. Thus (3) is called a model structure when viewed as a function of  $\theta$ .

The main result of [22] can now be stated as follows.

**Lemma 1** ([22]). Consider the feedback system (1)-(2) subject to Condition 1, and the model (3) subject to Condition 2. Consider  $V_N(\theta)$  given by (4). Then

$$\sup_{\theta \in \mathcal{D}} |V_N(\theta) - E[V_N(\theta)]| \rightarrow 0 \quad \text{w.p. 1 as } N \rightarrow \infty$$

## 2.2 Contracting discrete-time dynamics

Neuronal systems are most commonly represented by state-space models, and so we will rely on the state-space

formalism of contraction theory [25] to analyze the identification problem. We present both the discrete-time and continuous-time definitions in sequence, as they are both relevant to us.

First, consider the discrete-time system

$$x_{k+1} = f(x_k, u_k) \quad (9a)$$

$$y_k = h(x_k, u_k) \quad (9b)$$

where  $f$  and  $h$  are continuously differentiable functions,  $u : \mathbb{Z}_+ \rightarrow \mathbb{R}^{n_u}$  is the input signal,  $y : \mathbb{Z}_+ \rightarrow \mathbb{R}^{n_y}$  is the output signal, and  $x : \mathbb{Z}_+ \rightarrow \mathbb{R}^{n_x}$  is the state vector. We denote by  $x_k = \phi_{k,s}(u, x_s)$  the solution of (9a) that starts at time  $s$  and is evaluated at time  $k \geq s$ , when (9a) is subject to the input sequence  $u = u_{[0,\infty]}$  and initial condition  $x_s$ .

**Definition 1** ([25]). The discrete-time dynamics (9a) is said to be exponentially contracting in a positively invariant set  $X \subseteq \mathbb{R}^{n_x}$ , uniformly on  $U \subseteq \mathbb{R}^{n_u}$ , if there exist a symmetric matrix sequence  $P_k(x_k) \geq \epsilon I > 0$  and a constant  $\alpha < 1$  such that

$$\frac{\partial f^\top}{\partial x} P_{k+1} \frac{\partial f}{\partial x} \leq \alpha^2 P_k \quad (10)$$

for all  $k \in \mathbb{Z}_+, x_k \in X$ , and  $u_k \in U$ .

For brevity, when we say that a dynamics is exponentially contracting in a set, we implicitly require that the set be positively invariant.

The result below will be instrumental in connecting the contraction property to the PEM conditions of the previous section. For simplicity, we work with a constant contraction metric.

**Lemma 2.** Consider the discrete-time system (9). Let

$$y_k = F_k(u_{[0,k]}; x_0) = h(\phi_{k,0}(u, x_0), u_k) \quad (11)$$

For some  $\beta > 0$ , assume (9a) is exponentially contracting in a convex, closed and bounded set  $X$ , uniformly on  $U = [-\beta, \beta]^{n_u}$ , with a constant metric  $P > 0$ . Then there are  $C_1, C_2 > 0$  such that

$$\begin{aligned} & \|F_k(u_{[0,k]}; x_0) - F_k(\tilde{u}_{[0,k]}; \tilde{x}_0)\| \\ & \leq C_1 \sum_{m=0}^k \alpha^{k-m} \|u_m - \tilde{u}_m\| + C_2 \alpha^k \|x_0 - \tilde{x}_0\| \end{aligned} \quad (12)$$

for all  $k \geq 0, u, \tilde{u} \in \mathcal{U}_\beta^{n_u}$ , and  $x_0, \tilde{x}_0 \in X$ .

*Proof.* See the Appendix A.1.  $\square$

### 2.3 Contracting continuous-time dynamics

Consider the continuous-time nonlinear system

$$\dot{x}(t) = f(x(t), u(t)) \quad (13)$$

where  $f$  is a continuously differentiable function,  $u : \mathbb{R}_+ \rightarrow \mathbb{R}^{n_u}$  is an input signal and  $x : \mathbb{R}_+ \rightarrow \mathbb{R}^{n_x}$  is the state vector.

**Definition 2.** The continuous-time dynamics (13) is said to be exponentially contracting in a positively invariant set  $X \subseteq \mathbb{R}^{n_x}$ , uniformly on  $U \in \mathbb{R}^{n_u}$ , if there exists a continuously differentiable symmetric matrix  $P(x(t), t) \geq \epsilon I > 0$  and a constant  $\lambda > 0$  such that

$$\frac{\partial f^\top}{\partial x} P + P \frac{\partial f}{\partial x} + \dot{P} \leq -2\lambda P \quad (14)$$

for all  $t \in \mathbb{R}_+$ ,  $x(t) \in X$ , and  $u(t) \in U$ .

Alternatively, by writing  $P = \Theta^\top \Theta$ , (14) can be written as  $\frac{1}{2} (F + F^\top) \leq -\lambda I$ , with

$$F = \left( \dot{\Theta} + \Theta \frac{\partial f}{\partial x} \right) \Theta^{-1},$$

## 3 Conductance-based models under feedback

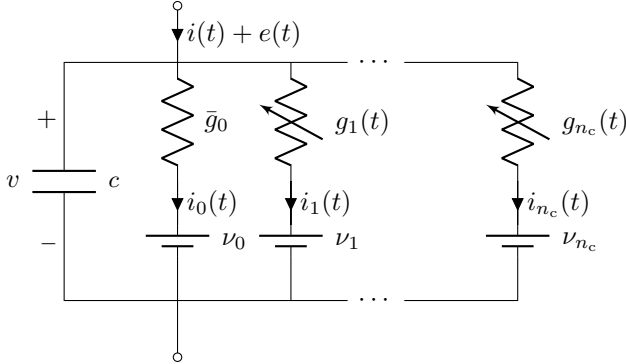


Fig. 2. Schematic representation of a neuronal system.

### 3.1 Conductance-based models

Conductance-based models are biophysical neuronal models that admit the circuit representation shown in Figure 2. While the framework of the present paper holds for multiple-input-multiple-output models, we focus on the single-input single-output case. Such models were first introduced in the seminal work of Hodgkin and Huxley [15]. For a general introduction, the reader is referred to Chapters 3 and 5 in [19], or textbooks of neurophysiology such as [14,18,9]. To date, conductance-based modeling remains the central paradigm of biophysically realistic neuronal modeling [1].

In a conductance-based model, the neuronal membrane is modeled by an ideal capacitor of capacitance  $c > 0$ . The voltage across the membrane, which is the output of the model, is given by  $v(t)$ . The neuron possesses  $n_c \in \mathbb{N}$  different types of ion channels embedded in its membrane. The ion channels allow ionic currents to flow across the membrane according to Kirchhoff's law,

$$c \dot{v}(t) = - \sum_{j=0}^{n_c} i_j(t) + i(t) + e(t) \quad (15)$$

where each current  $i_j(t)$ ,  $j = 1, \dots, n_c$ , models an ionic current. The ionic currents not explicitly included in the model are lumped in a leak current  $i_0(t)$ . In addition, the membrane voltage is affected by an external input current  $i(t)$  and an additive noise current  $e(t)$ . The noise current aggregates the effects of ion channel fluctuations [13] and background neuronal activity [12, Chapter 8].

All currents in a conductance-based model obey Ohm's law. The leak current

$$i_0(t) = \bar{g}_0(v(t) - \nu_0) \quad (16)$$

is characterized by a constant conductance  $\bar{g}_0 > 0$  and a constant reversal potential  $\nu_0 \in \mathbb{R}$ . In contrast, the conductances of the ionic currents are voltage-dependent. This dependence is the key source of nonlinearity of conductance-based models. Owing to the original proposal of Hodgkin and Huxley, each ionic current has a nonlinear state-space model of the form

$$\dot{m}_j = \frac{1}{\tau_{m,j}(v)} (-m_j + m_{\infty,j}(v)), \quad (17a)$$

$$\dot{h}_j = \frac{1}{\tau_{h,j}(v)} (-h_j + h_{\infty,j}(v)), \quad (17b)$$

$$i_j(t) = \bar{g}_j m_j^{\alpha_j}(t) h_j^{\beta_j}(t) (v(t) - \nu_j) \quad (17c)$$

with  $j = 1, \dots, n_c$ . The constants  $\bar{g}_j > 0$  are called the maximal conductances, and  $\nu_j \in \mathbb{R}$  are called reversal potentials. The variables  $m_j$  and  $h_j$  are called gating variables, and take values in the closed interval  $[0, 1]$ . Their dynamics are defined by the continuously differentiable functions

$$\tau_{m,j}, \tau_{h,j} : \mathbb{R} \rightarrow [\tau_{\min}, \tau_{\max}] \subset \mathbb{R}_+$$

and

$$m_{\infty,j}, h_{\infty,j} : \mathbb{R} \rightarrow [0, 1]$$

where  $\tau_{\min} > 0$ . The gating variables modulate the current conductance with a voltage-dependent first-order lag dynamics. The exponents  $\alpha_j$  and  $\beta_j$  belong to  $\mathbb{Z}_+$ , and whenever  $\alpha_{j^*} = 0$  or  $\beta_{j^*} = 0$ , we ignore (17a) or (17b) for  $j = j^*$ , respectively. These exponents, along with the gating variable dynamics (17a)-(17b), constitute the *kinetic model* of the  $j^{\text{th}}$  ion channel [19,14].

A compact representation of the entire model (15)-(17) has the state-space structure

$$c\dot{v} = -g(v, x) + i + e \quad (18a)$$

$$\dot{x} = A(v)x + b(v) \quad (18b)$$

where the vector  $x \in X = [0, 1]^{n_x}$  collects all the gating variables  $m_j$  and  $h_j$  for which  $\alpha_j > 0$  and  $\beta_j > 0$ , respectively, and

$$g(v, x) = \bar{g}_0(v - v_0) + \sum_{j=1}^{n_c} \bar{g}_j m_j^{\alpha_j} h_j^{\beta_j} (v - v_j) \quad (19)$$

denotes the total membrane internal current. Note that the matrix  $A(v)$  is diagonal, and  $b(v)$  is a vector-valued function of  $v$ . The model (18) is in the standard normal form of nonlinear minimum phase systems [4]: Kirchoff's equation (18a) is the input-output equation of a relative degree one model, and the gating dynamics (18b) are the system's internal dynamics.

**Example 1.** The Hodgkin-Huxley (HH) model [15] is the prototypical conductance-based model. It is given by (15), with  $c = 1 \mu\text{F}/\text{cm}^2$ , and it has two ionic currents ( $n_c = 2$ ): a sodium current  $i_{\text{Na}}$ , and a potassium current  $i_{\text{K}}$ . It also includes a leak current  $i_{\text{L}}$ . The currents are given by

$$\begin{aligned} i_0 &= i_{\text{L}} = 0.3(v + 54.4) \\ i_1 &= i_{\text{Na}} = 120 m_{\text{Na}}^3 h_{\text{Na}} (v - 55) \\ i_2 &= i_{\text{K}} = 36 m_{\text{K}}^4 (v + 77) \end{aligned} \quad (20)$$

The three internal variables are the sodium activation  $m_1 = m_{\text{Na}}$ , sodium inactivation  $h_1 = h_{\text{Na}}$ , and potassium activation  $m_2 = m_{\text{K}}$  (there is no potassium inactivation in the model, i.e.,  $\beta_2 = 0$ ). The vector  $x$  collecting these variables is given by  $x = (m_1, h_1, m_2)^\top = (m_{\text{Na}}, h_{\text{Na}}, m_{\text{K}})^\top$ . The different voltage dependent time-constants  $\tau(v)$  and activation functions  $m_\infty(v)$  and  $h_\infty(v)$  are illustrated in Figures 3 and 4, respectively, and are detailed in Appendix B.

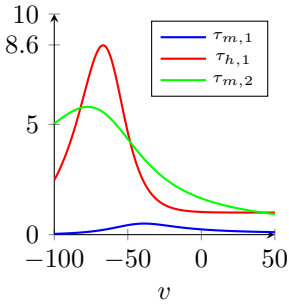


Fig. 3. Time constant functions  $\tau_{m,j}$  and  $\tau_{h,j}$  in the Hodgkin-Huxley model.

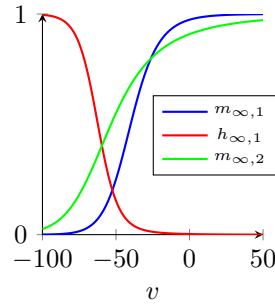


Fig. 4. Nonlinear activation functions  $m_{\infty,j}$  and  $h_{\infty,j}$  in the Hodgkin-Huxley model.

Each gating variable remains in the interval  $[0, 1]$ , and, in the absence of external inputs, the voltage remains in the interval  $[\nu_2, \nu_1] = [\nu_{\text{K}}, \nu_{\text{Na}}] = [-77, 55]$ . This is illustrated in Figure 5, where a *spiking* limit cycle oscillation occurs in response to a small constant input.

The internal dynamics (18b) of the Hodgkin-Huxley model in Example 1 are exponentially contracting in  $[0, 1]^3$ , uniformly on  $V = \mathbb{R}$  (Definition 2). This is verified with the constant metric  $P = pI$ , for any  $p > 0$ , and any  $\lambda$  such that  $0 < \lambda < 1/\tau_{\text{max}}$ : in that case, we have

$$-2p \text{diag} \left( \frac{1}{\tau_{m,1}(v)}, \frac{1}{\tau_{h,1}(v)}, \frac{1}{\tau_{m,2}(v)} \right) \leq -\frac{2}{\tau_{\text{max}}} pI$$

and we could pick, for instance,  $\lambda < 1/8.6$  (see Figure 3). This is in fact a general property of conductance-based models:

**Proposition 1.** The conductance-based model (18) has a global relative degree of one, and is globally minimum phase (in the sense of [4]). The internal dynamics are exponentially contracting in  $x \in [0, 1]^{n_x}$ , uniformly on  $V = \mathbb{R}$ : there is a  $P_x > 0$  and a  $\lambda_x > 0$  such that

$$P_x A(v(t)) + A(v(t))^\top P_x \leq -2\lambda_x P_x \quad (21)$$

for all  $v(t) \in \mathbb{R}$ .

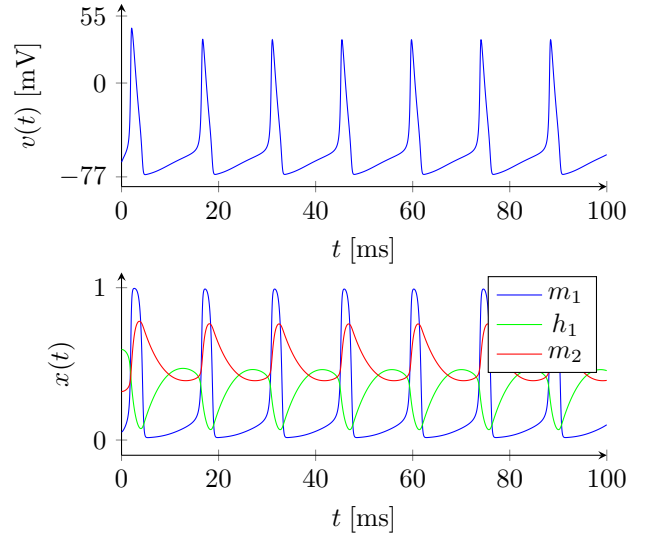


Fig. 5. Simulated state trajectories of Hodgkin-Huxley model (Example 1) for  $i(t) = 10 \mu\text{A}/\text{cm}^2$ ,  $e(t) = 0 \mu\text{A}/\text{cm}^2$ .

### 3.2 Output feedback contraction

A direct consequence of Proposition 1 is that a conductance-based model has a stable inverse. More precisely, using a static output feedback law, the closed-loop dynamics can be made exponentially contracting:

**Proposition 2.** Consider a conductance-based model (18) subject to the output feedback law

$$i(t) = \gamma(r(t) - v(t)) \quad (22)$$

where  $\gamma > 0$  is a constant gain and  $r(t)$  is a reference signal. Assume  $|r(t)|, |e(t)| < \beta$  for all  $t \geq 0$ . Let

$$V_{\beta, \gamma} = \left[ \min_j \left\{ \nu_j, -\frac{\beta(\gamma+1)}{\gamma} \right\}, \max_j \left\{ \nu_j, \frac{\beta(\gamma+1)}{\gamma} \right\} \right] \quad (23)$$

Then  $V_{\beta, \gamma} \times [0, 1]^{n_x}$  is a positively invariant set for the closed-loop dynamics (18), (22), and there exists a  $\gamma > 0$  such that the dynamics is exponentially contracting in  $V_{\beta, \gamma} \times [0, 1]^{n_x}$ , uniformly on  $[-\beta, \beta]^2$ .

*Proof.* First, to see that  $V_{\beta, \gamma} \times [0, 1]^{n_x}$  is a positively invariant set for any  $\beta, \gamma > 0$ , note that  $x \in [0, 1]^{n_x}$  implies  $\bar{g}_j m_j^{\alpha_j} h_j^{\beta_j} \geq 0$  in (17c). Then, it suffices to check that  $\dot{v} \geq 0$  for  $v = \min_j \{ \nu_j, -\beta(\gamma+1)/\gamma \}$ , and  $\dot{v} \leq 0$  for  $v = \max_j \{ \nu_j, \beta(\gamma+1)/\gamma \}$ .

We now follow an argument similar to [33, Section 2.2]. The Jacobian (with respect to the states) of the closed-loop dynamics (18), (22) is given by

$$J = \begin{bmatrix} -\frac{1}{c} \left( \frac{\partial g}{\partial v} + \gamma \right) & -\frac{1}{c} \frac{\partial g}{\partial x} \\ \frac{\partial A}{\partial v} x + \frac{\partial b}{\partial v} & A(v) \end{bmatrix}$$

(we omit dependencies on  $x$  and  $v$  for clarity). By Proposition 1, the internal dynamics (18b) has a contraction metric  $P_x = \Theta_x^\top \Theta_x > 0$  associated with the rate  $\lambda_x > 0$ . We will use the matrix

$$\Theta = \begin{bmatrix} c & 0 \\ 0 & \Theta_x \end{bmatrix}$$

to define a contraction metric  $P = \Theta^\top \Theta$  for the closed-loop system. Define  $F = \Theta J \Theta^{-1}$  (this is the generalized Jacobian of the closed-loop system). Then

$$F = \begin{bmatrix} F_{11} & -\frac{\partial g}{\partial x} \Theta_x^{-1} \\ \frac{1}{c} \Theta_x \left( \frac{\partial A}{\partial v} x + \frac{\partial b}{\partial v} \right) & F_{22} \end{bmatrix}$$

with

$$F_{11} = -\frac{1}{c} \left( \frac{\partial g}{\partial v} + \gamma \right) \quad (24)$$

and

$$F_{22} = \Theta_x A(v) \Theta_x^{-1} \quad (25)$$

We will use  $F \prec 0$  to denote  $\frac{1}{2}(F + F^\top) \leq -\epsilon I$  for all  $t \geq 0$ ,  $(v, x) \in V_{\beta, \gamma} \times [0, 1]^{n_x}$ , and some  $\epsilon > 0$ . By Definition 2, to demonstrate contraction of the closed-loop system, we have to show that  $F \prec 0$ . To do that,

we will require that  $F_{11} \prec 0$  and  $F_{22} \prec 0$ . Contraction of the internal dynamics (see (21)) automatically implies

$$\frac{1}{2} (F_{22} + F_{22}^\top) \leq -\lambda_x I \quad (26)$$

and thus  $F_{22} \prec 0$ . Furthermore,

$$\frac{\partial g}{\partial v}(v, x) = g_0 + \sum_{j=1}^{n_c} \bar{g}_j m_j^{\alpha_j} h_j^{\beta_j} \geq g_0 > 0 \quad (27)$$

and thus  $F_{11} \prec 0$  as well. Since  $F_{11} \prec 0$ , by a standard Schur complement result [16, pp. 472], we have  $F \prec 0$  if and only if

$$\frac{1}{2} (F_{22} + F_{22}^\top) < Q^\top F_{11}^{-1} Q \quad (28)$$

where  $Q$  is the row vector given by

$$Q = \frac{1}{2} \left( -\frac{\partial g}{\partial x} \Theta_x^{-1} + \frac{1}{c} \left( \frac{\partial A}{\partial v} x + \frac{\partial b}{\partial v} \right)^\top \Theta_x^\top \right) \quad (29)$$

From (24), (27), (26) and (28),  $F \prec 0$  if and only if

$$\gamma I > c \left[ -\frac{1}{2} (F_{22} + F_{22}^\top) \right]^{-1} Q^\top Q - \frac{\partial g}{\partial v} \quad (30)$$

By (26) and (27), a sufficient condition for (30) to hold is

$$\gamma > \frac{c}{\lambda_x} \sigma_{\max}[Q]^2 \quad (31)$$

where  $\sigma_{\max}[Q]$  is the largest singular value of  $Q$ .

Since the continuous functions  $\partial g/\partial x$ ,  $\partial A/\partial v$  and  $\partial b/\partial v$  in (29) are bounded on  $V_{\beta, \gamma} \times [0, 1]^{n_x}$  for any  $\beta, \gamma > 0$ , it follows that  $\sigma_{\max}[Q]$  is also bounded on that set. Since  $V_{\beta, \gamma_2} \subseteq V_{\beta, \gamma_1}$  for  $\gamma_2 \geq \gamma_1$ , the maximum of  $\sigma_{\max}[Q]$  on  $V_{\beta, \gamma} \times [0, 1]^{n_x}$  is non-increasing in  $\gamma$ . Thus, a sufficiently large  $\gamma$  ensures that (31) is satisfied.  $\square$

The expressions (30) and (31) can be used to estimate a bound on the gain that is necessary to stabilize the conductance-based model. Depending on the choice of the contraction metric  $P_x$ , this bound can of course be conservative, as illustrated by the following example.

**Example 2.** For the Hodgkin-Huxley model (Example 1), choose  $P_x = I$  and  $\lambda_x = 1/8.6 < 1/\tau_{\max}$ . Consider the set  $[-77, 55] \subseteq V_{\beta, \gamma}$ . Computing the right-hand side of (30) for  $v = -77$ ,  $m_1 = h_1 = m_2 = 1$ , and  $\Theta_x = I$ , leads to the bound  $5.1 \times 10^8$  mS/cm<sup>2</sup> the gain necessary to ensure exponential contraction of the closed-loop system. Alternatively, consider the contraction metric  $P_x = 10^6 \times \text{diag}(0.21, 3.80, 3.16)$ . In this case, a random search over the set  $[-77, 55] \times [0, 1]^3$  gives a less conservative bound of (30) of  $2.7 \times 10^3$  mS/cm<sup>2</sup>.

### 3.2.1 Non-ohmic ion currents

The Ohmic expression of the ionic current (17c) is not necessary for the output feedback contraction property of the model. Instead of the Ohmic ionic current (17c), we could have used the more general formulation

$$i_j = \bar{g}_j m_j^{\alpha_j} h_j^{\beta_j} p_j(v)$$

with

$$p_j(v) = \sum_{\ell=0}^{d_j} \eta_\ell v^\ell$$

where each  $d_j$  is an arbitrarily large polynomial degree, and  $\eta_\ell \in \mathbb{R}$ . In most non-Ohmic ionic current models,  $p_j(v)$  is a monotonically increasing function (see, e.g., [19, Chapter 3]), and the reversal potential  $\nu_j \in \mathbb{R}$  is the value where  $p(\nu_j) = 0$ . In this case,

$$\text{sign}(p_j(v)) = \text{sign}(v - \nu_j) \quad (32)$$

where by convention  $\text{sign } 0 = 0$ . Thus  $V_{\beta,\gamma} \times [0, 1]^{n_x}$ , with  $V_{\beta,\gamma}$  given by (23), remains a positively invariant set under the more general ionic current model above. Since the vast majority of ionic current models is Ohmic, we keep the formulation (17c), noting that all the results in this paper can be easily adapted to allow for the non-Ohmic case above.

### 3.3 The voltage-clamp experiment

The output contraction property of conductance-based models is a consequence of the very experimental protocol that has been used to identify neuronal systems in the past: the voltage-clamp experiment, pioneered by Hodgkin and Huxley. The voltage-clamp experiment is nothing but a high-gain output feedback experimental protocol employed to stabilize the neuron and to determine its inverse dynamics through step response experiments. The principle of that experiment is illustrated in Figure 6. In the limit of high-gain feedback, the current drawn from the amplifier to clamp the voltage to the reference  $r(t)$  is by definition the output of the internal dynamics driven by the voltage  $v(t) = r(t)$ . Electrophysiologists rely on the stability of that inverse system to model the internal dynamics through a series of step responses. In that sense, the contraction property of conductance-based models is an experimental property of neurons rather than the property of a specific mathematical model of the ionic currents.

Models of specific ion channel types have been accumulated over time by electrophysiologists. Today, online databases such as ModelDB [27] contain large libraries of ion channels models. The structure of those models is often used in parametric identification of new types of

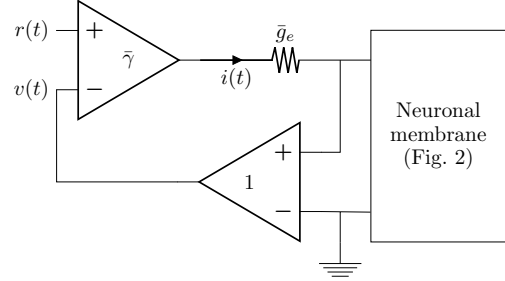


Fig. 6. The voltage-clamp experiment: electrodes are used to inject the current  $i(t)$  and measure the voltage  $v(t)$  of the neuronal membrane. The amplifiers are ideal differential amplifiers, and  $\bar{g}_e$  models the electrode conductance. When  $\bar{\gamma} \gg 1$ , this implements the feedback law (22) with  $\gamma = \bar{\gamma}\bar{g}_e$ .

neurons (see, e.g., [8,17]). The identified parameters include the maximal conductances  $\bar{g}_j$  and the Nernst potentials  $\nu_j$ . The purpose of the next sections will be to show that, the classical PEM provides consistent estimates for these parameters.

### 3.4 Discretized conductance-based models

The data obtained for identification purposes is in the form of a discrete sequence of samples. In the next sections, we will consider simple discretizations of (18) resulting from the forward-Euler method:

$$v_{k+1} = v_k + \frac{t_s}{c} (-g(v_k, x_k) + i_k + e_k) \quad (33a)$$

$$x_{k+1} = x_k + t_s (A(v_k)x_k + b(v_k)), \quad (33b)$$

where  $t_s > 0$  is the sampling period.

The following result shows that such discretization retains the contraction property of the continuous-time model.

**Lemma 3.** Assume that the continuous-time dynamics (13) is exponentially contracting in a closed and bounded set  $X$ , uniformly on  $[-\beta, \beta]^{n_u}$  (with  $\beta > 0$ ), with a constant metric  $P$ . Let

$$x_{k+1} = x_k + t_s f(x_k, u_k) \quad (34)$$

where  $t_s > 0$  is the sampling period. Then there exists a sufficiently small  $t_s$  such that the discrete-time dynamics (34) is exponentially contracting in  $X$ , uniformly on  $[-\beta, \beta]^{n_u}$ .

*Proof.* See the Appendix A.2.  $\square$

## 4 Identification of neuronal models with the PEM

In this section, we discuss the parametric identification of conductance-based models. In Section 4.1, we define

the identification setup, and in Section 4.2, we treat the case in which we can consistently identify the system's maximal conductances and reversal potentials by solving a linear least-square optimization problem.

#### 4.1 Identification setup

The system (33) under the feedback law  $i_k = \gamma(r_k - v_k)$  can be written in the form

$$x_{k+1} = x_k + t_s (A(u_{2,k})x_k + b(u_{2,k})) \quad (35a)$$

$$y_k = \frac{1}{c} (g(u_{2,k}, x_k) - u_{1,k} - e_k) \quad (35b)$$

and

$$v_{k+1} = v_k - t_s y_k \quad (36a)$$

$$u_k = \begin{bmatrix} u_{1,k} \\ u_{2,k} \end{bmatrix} = \begin{bmatrix} \gamma(r_k - v_k) \\ v_k \end{bmatrix} \quad (36b)$$

where  $x$  collects the states  $m_j$  and  $h_j$  for which  $\alpha_j, \beta_j > 0$ ,  $A(\cdot)$  and  $b(\cdot)$  are determined by (17a)-(17b), and  $g(\cdot, \cdot)$  is given by (19). It can be seen that by backward iteration of (35a) and (36a), we can find a  $F_k$  and a  $H_k$  such that  $y_k$  and  $u_k$  can be represented by (1) and (2), respectively. Thus, the identification setup is represented by Figure 1.

**Assumption 1.** (Input-additive white noise) The input-additive noise  $e_k$  is a sequence of independent random variables such that  $E[e_k] = 0$ , and  $E[e_k^2] = \sigma_e^2 > 0$ . All realizations of  $e$  belong to  $\mathcal{U}_\beta$ .

**Assumption 2.** (Known signals) The signals  $r_k$  and  $v_k$  are known ( $v_k$  is measured without noise), and  $r$  is a deterministic signal that belongs to  $\mathcal{U}_\beta$ .

Assumption 2 is consistent with the voltage-clamp experiment: it allows for current noise but assumes that the voltage is perfectly measured.

**Assumption 3.** For  $r, e \in \mathcal{U}_\beta$ , the closed-loop dynamics (35)-(36) is exponentially contracting in  $V_{\beta,\gamma} \times [0, 1]^{n_x}$ , uniformly on  $[-\beta, \beta]^2$ , where  $V_{\beta,\gamma}$  is given by (23).

It follows directly from Proposition 2 and Lemma 3 that there is a large enough value of  $\gamma$ , and a small enough value of  $t_s$  (possibly depending on  $\gamma$ ) such that Assumption 3 is verified<sup>2</sup>.

The following result will help us apply the identification framework of Section 2.

<sup>2</sup> Notice that there is a tradeoff in the choice of the values of  $\gamma$  and  $t_s$ . Increasing the value of  $\gamma$  (which increases the size of  $\bar{\sigma}$  in (A.7)) might require decreasing the value of  $t_s$  so that contraction of the discrete-time system is preserved.

**Proposition 3.** Under Assumptions 1-3, the closed-loop system (35)-(36) satisfies Condition 1.

*Proof.* See the Appendix A.3.  $\square$

#### 4.2 Identification with fixed ion channel kinetics

A given library of ion channel kinetic models can be used in the identification of the parameters  $c$ ,  $\bar{g}_j$ , and  $\nu_j$  of a neuronal system (recall that an ion channel kinetic model is given by the dynamics (17a)-(17b), as well as the coefficients  $\alpha_j$ ,  $\beta_j$  in (17c)). This can be done by postulating a model structure containing  $n_m$  known ion channel kinetic models, chosen a priori. For  $j = 1, \dots, n_m$ , we denote the objects defining the model structure kinetic models by  $\hat{\tau}_{m,j}(\cdot)$ ,  $\hat{\tau}_{h,j}(\cdot)$ ,  $\hat{m}_{\infty,j}(\cdot)$ ,  $\hat{h}_{\infty,j}(\cdot)$ ,  $\hat{\alpha}_j$  and  $\hat{\beta}_j$ . The model structure states  $\hat{m}_j$  and  $\hat{h}_j$  evolve analogously to the discretized form of (17a)-(17b). These dynamics can be described in compact form by

$$\hat{x}_{k+1} = \hat{x}_k + t_s \left( \hat{A}(u_{2,k})\hat{x}_k + \hat{b}(u_{2,k}) \right) \quad (37)$$

where  $\hat{x}$  collects the gating variables  $\hat{m}_j$  and  $\hat{h}_j$  for which  $\hat{\alpha}_j > 0$  and  $\hat{\beta}_j > 0$ , respectively.

The unknown parameters of the true system,  $c$ ,  $\bar{g}_j$ , and  $\nu_j$ , all appear in the right-hand side of (35b), either directly or through the mapping  $g(\cdot, \cdot)$  given by (19). To identify those parameters, we define the model structure output  $\hat{y}_k(\theta)$  by

$$\hat{y}_k(\theta) = \sum_{j=1}^{n_m} (\theta_j^{(1)} + \theta_j^{(2)} u_{2,k}) \hat{m}_{j,k}^{\hat{\alpha}_j} \hat{h}_{j,k}^{\hat{\beta}_j} + \theta_0^{(1)} + \theta_0^{(2)} u_{2,k} + \theta^{(3)} u_{1,k} \quad (38)$$

where  $u_{1,k}$  and  $u_{2,k}$  are the elements of the model structure input in (36b), and where the vector of model structure parameters  $\theta \in \mathcal{D} \subseteq \mathbb{R}^{(2n_m+1) \times 1}$  has been partitioned according to

$$\theta = (\theta^{(1)\top}, \theta^{(2)\top}, \theta^{(3)\top})^\top$$

with  $\theta^{(1)} \in \mathbb{R}^{n_m \times 1}$ ,  $\theta^{(2)} \in \mathbb{R}^{n_m \times 1}$  and  $\theta^{(3)} \in \mathbb{R}$ .

We can more compactly write

$$\hat{y}_k(\theta) = \psi_k \theta$$

with the row vector  $\psi_k \in \mathbb{R}^{1 \times (2n_m+1)}$  given by

$$\psi_k = \left( 1, \hat{m}_{1,k}^{\hat{\alpha}_1} \hat{h}_{1,k}^{\hat{\beta}_1}, \dots, \hat{m}_{n_m,k}^{\hat{\alpha}_{n_m}} \hat{h}_{n_m,k}^{\hat{\beta}_{n_m}}, u_{2,k}, u_{2,k} \hat{m}_{1,k}^{\hat{\alpha}_1} \hat{h}_{1,k}^{\hat{\beta}_1}, \dots, u_{2,k} \hat{m}_{n_m,k}^{\hat{\alpha}_{n_m}} \hat{h}_{n_m,k}^{\hat{\beta}_{n_m}}, u_{1,k} \right)$$

Gathering  $\psi_k$  in a matrix  $\Psi_N \in \mathbb{R}^{(N+1) \times (2n_m+1)}$  given by

$$\Psi_N = [\psi_N^\top, \psi_{N-1}^\top, \dots, \psi_0^\top]^\top \quad (39)$$

we find that the vector of model structure outputs from time  $k = N$  down to time  $k = 0$  is given by

$$\hat{y}_{[0,N]}^\top(\theta) = \Psi_N \theta$$

The above formulation shows that the ion channel kinetic models act as basis operators mapping the input sequence  $u_{[0,N]}$ , given by (36b), to the columns of  $\Psi_N$ . Using that formulation, we will make some assumptions in order to show that we can obtain consistent estimates of the parameter vector  $\theta$  using the PEM.

First, we need all the true ion channels to be included in the model structure:

**Assumption 4.** The model structure contains the true system (35): for  $j = 1, \dots, n_c \leq n_m$ , we have  $\hat{\tau}_{m,j}(\cdot) = \tau_{m,j}(\cdot)$ ,  $\hat{\tau}_{h,j}(\cdot) = \tau_{h,j}(\cdot)$ ,  $\hat{m}_{\infty,j}(\cdot) = m_{\infty,j}(\cdot)$ ,  $\hat{h}_{\infty,j}(\cdot) = h_{\infty,j}(\cdot)$ ,  $\hat{\alpha}_j = \alpha_j$  and  $\hat{\beta}_j = \beta_j$ .

In case Assumption 4 is verified, then the true parameter vector, which we denote by  $\bar{\theta} = (\bar{\theta}^{(1)\top}, \bar{\theta}^{(2)\top}, \bar{\theta}^{(3)\top})^\top$ , is given by

$$\begin{aligned} \bar{\theta}_j^{(1)} &= \begin{cases} -\bar{g}_j \nu_j / c, & j = 0, 1, \dots, n_c \\ 0, & j > n_c \end{cases} \\ \bar{\theta}_j^{(2)} &= \begin{cases} \bar{g}_j / c, & j = 0, 1, \dots, n_c \\ 0, & j > n_c \end{cases} \\ \bar{\theta}^{(3)} &= -1/c \end{aligned} \quad (40)$$

We will also need the following standard assumption:

**Assumption 5** (Persistence of excitation). There is a  $N^* > 0$  such that  $\frac{1}{N} \Psi_N^\top \Psi_N$  and  $E \left[ \frac{1}{N} \Psi_N^\top \Psi_N \right]$  are positive-definite for all  $N > N^*$ .

Assumption 5 is an assumption both on the model structure and on  $r_k$ , the signal used to excite the true system. Intuitively, we should not include two identical ion channel kinetics in the model structure, and the excitation signal  $r_k$  should be sufficiently rich.

Finally, we make a last assumption in order to simplify our result:

**Assumption 6.** The initial states of the true system and of the model structure satisfy  $\hat{m}_{j,0} = m_{j,0}$  and  $\hat{h}_{j,0} = h_{j,0}$  for  $j = 1, \dots, n_c$ .

In principle, we could also estimate initial conditions. However, given the contracting nature of the ion channel kinetics considered here, initial conditions are forgotten exponentially fast. As long as Assumption 4 is verified, we can come arbitrarily close to verifying Assumption 6 by discarding initial segments of the data.

Under Assumption 2, we are able to compute

$$y_k = -\frac{v_{k+1} - v_k}{t_s}$$

from the measurements, and thus we can form the cost function  $V_N(\theta)$  given by (4). We can now state the following result.

**Theorem 1.** Let Assumptions 1-6 be satisfied. Let  $N > N^*$ , and let  $\hat{\theta}_N = (\hat{\theta}_N^{(1)\top}, \hat{\theta}_N^{(2)\top}, \hat{\theta}_N^{(3)\top})^\top$  be given by

$$\begin{aligned} \hat{\theta}_N &= \arg \min_{\theta \in \mathcal{D}} V_N(\theta) \\ &= \arg \min_{\theta \in \mathcal{D}} \frac{1}{N} \|y_{[0,N]}^\top - \Psi_N \theta\|_2^2 \end{aligned} \quad (41)$$

where  $y_k$  and  $\Psi_N$  are given by (35b) and (39), respectively, and  $\mathcal{D}$  is a compact parameter domain containing  $\bar{\theta}$ , the true parameter vector (40). Then, we have  $\hat{\theta}_N \rightarrow \bar{\theta}$  w.p. 1 as  $N \rightarrow \infty$ .

*Proof.* By Assumptions 4 and 6, the true output  $y_k$ , given by (35b) (see also (19)), can be written as

$$y_{[0,N]}^\top = \Psi_N \bar{\theta} - \frac{1}{c} e_{[0,N]}^\top$$

and thus we can write

$$E[V_N(\theta)] = \frac{1}{N} E \left[ \|\Psi_N(\bar{\theta} - \theta) - \frac{1}{c} e_{[0,N]}^\top\|_2^2 \right]$$

By Assumption 1, the time-delay present in the system ensures that  $v_k$  and  $x_k$  do not depend on  $e_k$ . We then have that

$$E \left[ \Psi_N^\top e_{[0,N]}^\top \right] = 0$$

and thus

$$E[V_N(\theta)] = \frac{1}{N} (\bar{\theta} - \theta)^\top E \left[ \Psi_N^\top \Psi_N \right] (\bar{\theta} - \theta) + \frac{1}{c} \sigma_e^2$$

Using Assumption 5, we have

$$\arg \min_{\theta \in \mathcal{D}} E[V_N(\theta)] = \bar{\theta} \quad (42)$$

for all  $N > N^*$ .

It remains to show that  $\hat{\theta}_N$  converges to (42) w.p. 1 as  $N \rightarrow \infty$ , which can be done by means of Lemma 1. Condition 1 is satisfied due to Proposition 3. By Assumptions 2 and 3, the input (36b) to the model structure

belongs to  $\mathcal{U}_{\beta^*}^2$  for some  $\beta^* > 0$ , since  $v_k$  remains in the compact set  $V_{\beta, \gamma}$ . Proposition 1 and Lemma 2 then ensure that the model structure verifies Condition 2. It follows by Lemma 1 that  $V_N(\theta)$  converges uniformly to  $E[V_N(\theta)]$  on the compact set  $\mathcal{D}$ . In view of (41) and (42), this ensures the result of the theorem.  $\square$

## 5 Examples

In this section, we illustrate the results of Section 4.2 by identifying various discrete-time neuronal models. All discrete-time models are obtained by forward-Euler discretization of their continuous-time counterparts with  $t_s = 0.005$  ms.

**Example 3.** In this example, we identify the discretized Hodgkin-Huxley (HH) model of Example 1. We include in the model structure the two ion channel kinetics present in the true model, and identify the values of  $c$ ,  $\bar{g}_j$ , and  $\nu_j$  using the parameter vector  $\theta$ . From (20) and (38), we have the following true parameters:

$\bar{\theta}_0^{(1)}$	$\bar{\theta}_0^{(2)}$	$\bar{\theta}_1^{(1)}$	$\bar{\theta}_1^{(2)}$	$\bar{\theta}_2^{(1)}$	$\bar{\theta}_2^{(2)}$	$\bar{\theta}^{(3)}$
$0.3 \cdot 54.4$	$0.3$	$120 \cdot -55$	$120$	$36 \cdot 77$	$36$	$-1$

We simulated an identification experiment in which the discretized HH model is subject to output feedback with  $\gamma = 50$ . The model is excited by the user-defined input  $r_k = -45 + \tilde{r}_k$ , where  $\tilde{r}_k$  is given by white Gaussian noise of standard deviation  $\sigma_r = 100$  that is filtered by the zero-order hold discretization of the system  $10^2/(s+10)^2$ . The input noise  $e_k$  was generated with  $\sigma_e = 2.5$  and was truncated so that  $e_k = 100$  whenever  $e_k \geq 100$ . This setup resulted in a signal-to-noise ratio (between  $y_k$  and  $e_k$ ) of around 30.8 dB. To eliminate transient effects and satisfy Assumption 6 as close as possible, we eliminated the initial 0.5 seconds of measurement (corresponding to  $10^5$  samples) from all datasets.

Figure 7 shows the estimation error  $\bar{\theta} - \hat{\theta}_N$  for  $N = 5 \times 10^5$  to  $5 \times 10^6$  (corresponding to experiment times of 0.5 to 5 seconds) for 20 different realizations of the experiment, as well as their average. We can see from the figure that the estimates steadily converge to the true parameters.

**Example 4.** In this example, we illustrate how a library of pre-established set of ion channel kinetic models can be used to identify different neuronal models. We consider three models, all of which are based on a forward-Euler discretization of the system given by

$$\dot{v}(t) = -0.3(v(t) + 17) - \sum_{j=1}^4 i_j(t) + i(t) + e(t)$$

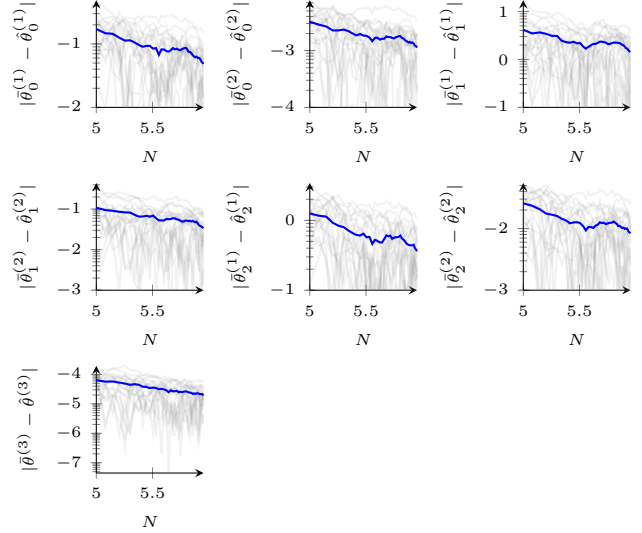


Fig. 7. The  $\log_{10} \times \log_{10}$  plots above show how the errors in the estimated parameters of Example 3 fall as the number of data points  $N$  increases. In grey: errors in each of the 20 realizations of the identification experiment as computed for  $N = 5 \times 10^5$  to  $5 \times 10^6$  ( $t_s = 0.005$ ). In blue: average of the 20 error traces.

with

$$\begin{aligned} i_1 &= 120 m_1^3 h_1(v - 55) \\ i_2 &= 20 m_2^4(v + 75) \\ i_3 &= \bar{g}_3 m_3^3 h_3(v + 75) \\ i_4 &= \bar{g}_4 m_4^2(v - 120) \end{aligned}$$

where the states  $m_j$  and  $h_j$  are given by (17a) and (17b), respectively with the functions  $m_{\infty, j}$ ,  $h_{\infty, j}$ ,  $\tau_{m, j}$  and  $\tau_{h, j}$  plotted in Figures 8-9 and described in Appendix C.

The above system, taken from [7], defines a modified version of the Connor-Stevens neuronal model [6]. The values of the variables  $\bar{g}_3$  and  $\bar{g}_4$  are the distinguishing factors between the three models we use in this example. We call them Connor-Stevens (CS) models A, B, and C, according to the following maximal conductance values:

CS model	A	B	C
$\bar{g}_3$	0	90	0
$\bar{g}_4$	0	0	0.4

Connor Stevens model A is similar to the HH model of the previous example, while models B and C differ from A due to the addition of ion currents  $i_3$  and  $i_4$ , respectively (these currents represent an ‘‘A-type’’ potassium current and a calcium current, respectively). It can be verified through simulations that the addition of  $i_3$  or  $i_4$  makes the qualitative input-output behavior (from  $i$  to  $v$ ) of models B and C differ from that of model A. In

particular, models B and C can fire periodic spikes with arbitrarily low frequency, while model A does not have that property (see, for instance, Figure 2 of [7]). The property of spiking with arbitrarily low frequency has important neurocomputational consequences. It underlies the classical distinction between Type I and Type II neuronal excitability first proposed by Hodgkin and Huxley (see [18, Chapter 7]).

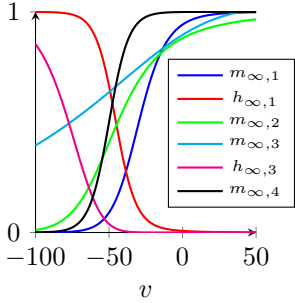


Fig. 8. Nonlinear activation functions  $m_{\infty,j}$  and  $h_{\infty,j}$  in the Connor-Stevens model.

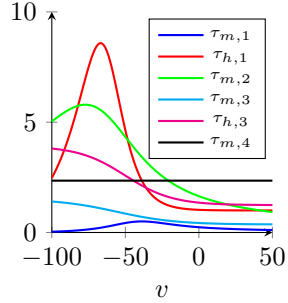


Fig. 9. Time constant functions  $\tau_{m,j}$  and  $\tau_{h,j}$  in the Connor-Stevens model.

To identify the models A, B and C, we include in a single model structure all four of the ion channels shared by those models. We simulated an identification experiment in which the discretized CS models are subject to output feedback with  $\gamma = 50$ . All models are excited by the user-defined input  $r_k = -45 + \tilde{r}_k$ , where  $\tilde{r}_k$  is given by white Gaussian noise of standard deviation  $\sigma_r = 30$  that is filtered by the zero-order hold discretization of the system  $10^2/(s + 10)^2$ . The input noise  $e_k$  was generated with  $\sigma_e = 1$  and was truncated so that  $e_k = 100$  whenever  $e_k \geq 100$ . This setup resulted in a signal-to-noise ratio (between  $y_k$  and  $e_k$ ) of around 28 dB, 26 dB and 29 dB for the CS models A, B and C, respectively (again, we eliminated the first 0.5 seconds of measurement from all datasets).

Figure 10 shows the evolution of the estimates of  $\bar{g}_j$  obtained by identifying each of the CS models A, B and C (for brevity, we do not show the evolution of all parameter estimates). It can be seen that the estimates of  $\bar{g}_3$  (or  $\bar{g}_4$ ) for models that do not contain  $i_3$  (or  $i_4$ ) tend towards zero, while the other estimates tend towards their true values.

## 6 Conclusion

In this paper, we studied the identification of neuronal systems under the assumption of current-additive zero-mean white noise and negligible voltage measurement noise. We showed that by treating a neuronal model as a closed-loop system, we can solve the identification problem by identifying the inverse dynamics with an output-error model structure. We have demonstrated

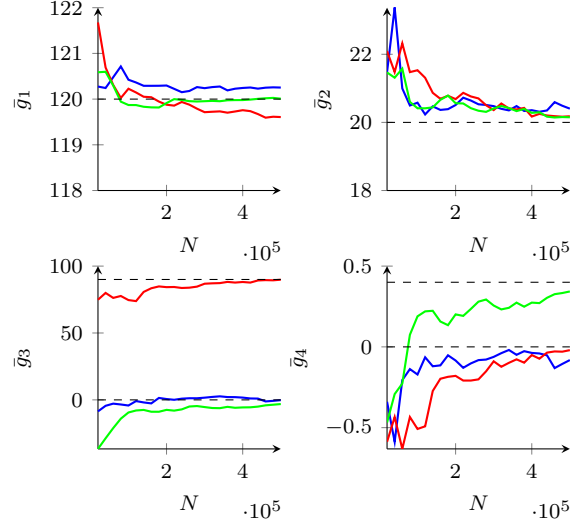


Fig. 10. Evolution of the estimates of  $\bar{g}_j$ , with respect to the number of samples, for each of the identified Connor-Stevens models A (blue), B (red) and C (green). The sampling period is  $t_s = 0.005$ , and the experimental setup is described in Example 4.

that consistent parameter estimates are obtained when the model structure contains the internal dynamics of the system being identified. This is a common strategy adopted in neuroscience, where kinetic models of ion channels are estimated in separate experiments (see, e.g., [27]). It is worth noting that the results in this paper may hold for ion channel models which are more general than (17a)-(17b); the key requirement is that the ion channels possess a contracting dynamics, so that (21) is satisfied. Thus, this work rigorously justifies neuronal system identification using conventional methods of nonlinear identification.

## Acknowledgements

This study was financed in part by the Coordenação de Aperfeiçoamento de Pessoal de Nível Superior – Brasil (CAPES) Finance Code 001. Maarten Schoukens is supported by the European Union’s Horizon 2020 research and innovation programme under the Marie Skłodowska-Curie Fellowship (grant agreement nr. 798627). The research leading to these results has received funding from the European Research Council under the Advanced ERC Grant Agreement Switchlet n.670645. The authors thank Monika Josza for her helpful comments on the manuscript.

## A Proofs

### A.1 Proof of Lemma 2

Let  $P = \Theta^\top \Theta$  ( $\Theta > 0$ ). For  $k \geq 0$ , let the sequences  $x_k$  and  $\tilde{x}_k$  be defined by the dynamics (9a) subject to

the inputs  $u_k$  and  $\tilde{u}_k$ , respectively. Applying the change of coordinates  $z_k = \Theta x_k$ , we obtain the discrete-time dynamics

$$z_{k+1} = f_\Theta(z_k, u_k) \quad (\text{A.1})$$

with  $f_\Theta$  given by

$$f_\Theta(\zeta, v) = \Theta f(\Theta^{-1}\zeta, v), \quad (\text{A.2})$$

The inequality (10) implies that

$$\sigma_{\max} \left[ \Theta \frac{\partial f}{\partial x}(x_k, u_k) \Theta^{-1} \right] \leq \alpha < 1 \quad (\text{A.3})$$

for all  $x_k \in X$  and  $k \in \mathbb{Z}_+$ . The inequality (A.3) in turn implies that the induced 2-norm of  $\partial f_\Theta / \partial \zeta$  satisfies  $\|\partial f_\Theta / \partial \zeta\|_2 \leq \alpha$  whenever

$$\zeta \in Z = \{\zeta \in \mathbb{R}^{n_x} \mid \zeta = \Theta \xi, \xi \in X\}$$

where (by convexity of  $X$ )  $Z$  is a convex set. Furthermore, since  $\partial f_\Theta / \partial v$  is a continuous function and  $Z \times [-\beta, \beta]^{n_u}$  is closed and bounded, there is some  $L_1 > 0$  such that  $\|\partial f_\Theta / \partial v\|_2 \leq L_1$  for all  $(\zeta, v) \in Z \times [-\beta, \beta]^{n_u}$ .

Now let  $\zeta, \tilde{\zeta} \in Z$  and  $v, \tilde{v} \in [-\beta, \beta]^{n_u}$ . Let also  $\gamma_1(s) = (1-s)\zeta + s\tilde{\zeta}$  and  $\gamma_2(s) = (1-s)\tilde{v} + sv$ , with  $s \in [0, 1]$ . It can be shown, using the mean value theorem (see, e.g., the proof of [20, Lemma 3.1]), that there is a  $s^* \in (0, 1)$  such that

$$\begin{aligned} \|f_\Theta(\zeta, v) - f_\Theta(\tilde{\zeta}, \tilde{v})\|_2 &\leq \left\| \frac{\partial f_\Theta}{\partial \zeta}(\gamma_1(s^*), \gamma_2(s^*))(\zeta - \tilde{\zeta}) \right. \\ &\quad \left. + \frac{\partial f_\Theta}{\partial v}(\gamma_1(s^*), \gamma_2(s^*))(v - \tilde{v}) \right\|_2 \end{aligned}$$

By convexity of  $Z \times [-\beta, \beta]^{n_u}$ , the above implies

$$\|f_\Theta(\zeta, v) - f_\Theta(\tilde{\zeta}, \tilde{v})\|_2 \leq \alpha \|\zeta - \tilde{\zeta}\|_2 + L_1 \|v - \tilde{v}\|_2 \quad (\text{A.4})$$

By recursive application of (A.1) and (A.4), we have

$$\|z_k - \tilde{z}_k\|_2 \leq L_1 \sum_{m=1}^k \alpha^{m-1} \|u_{k-m} - \tilde{u}_{k-m}\|_2 + \alpha^k \|z_0 - \tilde{z}_0\|_2$$

for  $k \geq 0$ . Multiplying both sides of the inequality by  $\|\Theta^{-1}\|_2$  and substituting  $z_k = \Theta x_k$ , we have

$$\begin{aligned} \|x_k - \tilde{x}_k\|_2 &\leq \frac{L_1}{\sigma_{\min}} \sum_{m=1}^k \alpha^{m-1} \|u_{k-m} - \tilde{u}_{k-m}\|_2 \\ &\quad + \frac{\sigma_{\max}}{\sigma_{\min}} \alpha^k \|x_0 - \tilde{x}_0\|_2 \end{aligned} \quad (\text{A.5})$$

for  $k \geq 0$ , where  $\sigma_{\max}$  and  $\sigma_{\min}$  denote the largest and the smallest singular values of  $\Theta$ , respectively.

By arguments similar to those used above, there are  $L_2, L_3 > 0$  such that

$$\|y_k - \tilde{y}_k\|_2 \leq L_2 \|x_k - \tilde{x}_k\|_2 + L_3 \|u_k - \tilde{u}_k\|_2 \quad (\text{A.6})$$

The result (12) follows directly from (A.6) and (A.5) by setting  $C_1 = \max\{(\alpha\sigma_{\min})^{-1}L_1L_2, L_3\}$  and  $C_2 = L_2\sigma_{\max}(\sigma_{\min})^{-1}$ .

### A.2 Proof of Lemma 3

Since  $\partial f / \partial x$  is continuous on the closed and bounded set  $X \times [-\beta, \beta]^{n_u}$ , there is a number  $\bar{\sigma}$  such that  $\bar{\sigma} \geq \sigma_{\max}[\partial f / \partial x]$  on that set. Let  $f_{t_s}(x_k, u_k) = x_k + t_s f(x_k, u_k)$ . Using (14), we have

$$\begin{aligned} \frac{\partial f_{t_s}^\top}{\partial x_k} P \frac{\partial f_{t_s}}{\partial x_k} &= \left(1 + t_s \frac{\partial f^\top}{\partial x_k}\right) P \left(1 + t_s \frac{\partial f}{\partial x_k}\right) \\ &\leq (1 - 2t_s\lambda)P + t_s^2 \frac{\partial f^\top}{\partial x_k} P \frac{\partial f}{\partial x_k} \\ &\leq \left(1 - 2t_s\lambda + t_s^2 \frac{\lambda_{\max}[P]}{\lambda_{\min}[P]} \bar{\sigma}^2\right) P \\ &= \alpha(t_s)^2 P \end{aligned} \quad (\text{A.7})$$

for all  $(x_k, u_k) \in X \times [-\beta, \beta]^{n_u}$ . The second inequality above is obtained using the fact that  $A^\top P A \leq \lambda_{\max}[P] \sigma_{\max}^2[A] I$  and  $I \leq 1/\lambda_{\min}[P] P$ . Making  $t_s < 1$  small enough ensures that  $\alpha(t_s)^2 < 1$ , and thus that the dynamics (34) is exponentially contracting on  $X$ , uniformly on  $[-\beta, \beta]^{n_u}$ .

### A.3 Proof of Proposition 3

Consider two different solutions of (35)-(36). The first is given by

$$\begin{aligned} (v_k, x_k^\top)^\top &= \phi_{k,0}(\gamma r + e, (v_0, x_0^\top)^\top) \\ (v_0, x_0^\top)^\top &= 0 \end{aligned} \quad (\text{A.8})$$

for  $k \geq 0$ , and the second is given by

$$\begin{aligned} (\bar{v}_{k,s+1}, \bar{x}_{k,s+1}^\top)^\top &= \phi_{k,s+1}(\gamma r + e, (\bar{v}_{s+1}, \bar{x}_{s+1}^\top)^\top) \\ (\bar{v}_{s+1}, \bar{x}_{s+1}^\top)^\top &= 0 \end{aligned} \quad (\text{A.9})$$

for  $k \geq s+1$ .

We will use the solutions above to construct the random variables  $\bar{y}_{k,s}$  involved in Condition 1. First, for each  $s \in \mathbb{Z}_+$ , we set  $\bar{y}_{s,s} = 0$ . From (35b), we compute the sequence  $y_k$  using (A.8), for  $k \geq 0$ , and the sequence

$\bar{y}_{k,s+1}$  using (A.9), for  $k \geq s+1$ . We have that  $\bar{y}_{k,s}$  is independent of  $e_{[0,s]}$ , since  $e_{[s+1,k]}$  is independent of  $e_{[0,s]}$ ; furthermore,  $r_k$  is deterministic; thus the independence required in Condition 1 is satisfied. We now need to verify (6a) for  $k \geq s$ . For  $k = s$ , we have

$$\begin{aligned} |y_s - \bar{y}_{s,s}| &= |y_s| = \frac{1}{c} |g(v_s, x_s) - \gamma(r_s - v_s) - e_s| \\ &\leq \frac{1}{c} (|g(v_s, x_s) + \gamma v_s| + (\gamma + 1)\beta) \\ &\leq C_1 \end{aligned} \quad (\text{A.10})$$

for some  $C_1 > 0$  and for each  $s \in \mathbb{Z}_+$ . To ensure this bound, we have used (from Assumptions 1 and 2) the fact that  $r, e \in \mathcal{U}_\beta$ , and the fact that  $g(v, x) + \gamma v$  is a continuous function on the compact  $V_{\beta,\gamma} \times [0, 1]^{n_x}$ .

Now, we make use of Assumption 3. Let  $\alpha_c < 1$  be the contraction rate of the closed-loop dynamics (35)-(36). Since  $|\gamma r + e| \leq (\gamma + 1)\beta$ , we can apply Lemma 2 (with the time origin shifted to  $s+1$ ) to see that there is a  $C_2 > 0$  such that

$$\begin{aligned} |y_k - \bar{y}_{k,s+1}| &\leq C_2 \alpha_c^{k-(s+1)} \|(v_{s+1}, x_{s+1}^\top) - (\bar{v}_{s+1}, \bar{x}_{s+1}^\top)\| \\ &= \alpha_c^{-1} C_2 \alpha_c^{k-s} \|(v_{s+1}, x_{s+1}^\top)\| \\ &\leq \alpha_c^{-1} C_2 C_3 \alpha_c^{k-s} \end{aligned} \quad (\text{A.11})$$

for each  $s \in \mathbb{Z}_+$  and  $k \geq s+1$ , where the constant  $C_3 > 0$  comes from the boundedness of  $V_{\beta,\gamma} \times [0, 1]^{n_x}$ . Taking  $E[\cdot^4]$  on both sides of (A.10) and (A.11), we verify (6a) with  $C = \max\{C_1^4, (\alpha_c^{-1} C_2 C_3)^4\}$  and  $\alpha = \alpha_c^4$ .

The random variables  $\bar{u}_{k,s}$  of Condition 1 can be constructed in a completely analogous way, and thus we omit this part of the proof.

## B Hodgkin-Huxley kinetic functions

To define the ion channel kinetics of the Hodgkin-Huxley model, we first set

$$\begin{aligned} \alpha_{m,1}(v) &= 0.1 \frac{-40 - v}{\exp\left(\frac{-40-v}{10}\right) - 1} & \beta_{m,1}(v) &= 4 \exp\left(\frac{-v-65}{18}\right) \\ \alpha_{h,1}(v) &= 0.07 \exp\left(\frac{-v-65}{20}\right) & \beta_{h,1}(v) &= \frac{1}{\exp\left(\frac{-35-v}{10}\right) + 1} \\ \alpha_{m,2}(v) &= 0.01 \frac{-55 - v}{\exp\left(\frac{-55-v}{10}\right) - 1} & \beta_{m,2}(v) &= 0.125 \exp\left(\frac{-v-65}{80}\right) \end{aligned}$$

Then, the functions  $\tau_{m,j}$  and  $m_{\infty,j}$ ,  $j = 1, 2$ , are given by

$$\begin{aligned} \tau_{m,j}(v) &= \frac{1}{\alpha_{m,j}(v) + \beta_{m,j}(v)} \\ m_{\infty,j}(v) &= \frac{\alpha_{m,j}(v)}{\alpha_{m,j}(v) + \beta_{m,j}(v)} \end{aligned} \quad (\text{B.1})$$

The same relationships are used to define  $\tau_{h,1}$  and  $h_{\infty,1}$ .

## C Connor-Stevens kinetic functions

The ion channel kinetics of the CS models are given by the relationships (B.1), with

$$\begin{aligned} \alpha_{m,1}(v) &= 0.38 \frac{-29.7 - v}{\exp\left(\frac{-29.7-v}{10}\right) - 1} & \beta_{m,1}(v) &= 15.2 \exp\left(\frac{-54.7-v}{18}\right) \\ \alpha_{h,1}(v) &= 0.266 \exp\left(\frac{-v-48}{20}\right) & \beta_{h,1}(v) &= 3.8 \frac{1}{\exp\left(\frac{-18-v}{10}\right) + 1} \\ \alpha_{m,2}(v) &= 0.019 \frac{-45.7 - v}{\exp\left(\frac{-45.7-v}{10}\right) - 1} & \beta_{m,2}(v) &= 0.2375 \exp\left(\frac{-55.7-v}{80}\right) \end{aligned}$$

The remaining functions are given by

$$\begin{aligned} \tau_{m,3}(v) &= 0.3632 + \frac{1.158}{(1 + \exp\left(\frac{v+55.96}{20.12}\right))} \\ m_{\infty,3}(v) &= \left(0.0761 \frac{\exp\left(\frac{v+94.22}{31.84}\right)}{1 + \exp\left(\frac{v+1.17}{28.93}\right)}\right)^{\frac{1}{3}} \\ \tau_{h,3}(v) &= 1.24 + \frac{2.678}{1 + \exp\left(\frac{v+50}{16.027}\right)} \\ h_{\infty,3}(v) &= \frac{1}{(1 + \exp\left(\frac{v+53.3}{14.54}\right))^4} \end{aligned}$$

and

$$\begin{aligned} \tau_{m,4}(v) &= 2.35 \\ m_{\infty,4}(v) &= \frac{1}{1 + \exp(-0.15(v + 50))} \end{aligned}$$

## References

- [1] Mara Almog and Alon Korngreen. Is realistic neuronal modeling realistic? *Journal of Neurophysiology*, 116(5):2180–2209, August 2016.
- [2] S. Boyd and L. Chua. Fading memory and the problem of approximating nonlinear operators with Volterra series. *IEEE Transactions on Circuits and Systems*, 32(11):1150–1161, November 1985.
- [3] Thiago Burghi, Maarten Schoukens, and Rodolphe Sepulchre. Feedback for nonlinear system identification. In *2019 18th European Control Conference (ECC)*, pages 1344–1349, June 2019.
- [4] C. I. Byrnes, A. Isidori, and J. C. Willems. Passivity, feedback equivalence, and the global stabilization of minimum phase nonlinear systems. *IEEE Transactions on Automatic Control*, 36(11):1228–1240, November 1991.
- [5] Raúl A. Casas, Robert R. Bitmead, Clas A. Jacobson, and C. Richard Johnson. Prediction error methods for limit cycle data. *Automatica*, 38(10):1753–1760, October 2002.
- [6] J A Connor, D Walter, and R McKown. Neural repetitive firing: modifications of the Hodgkin-Huxley axon suggested by experimental results from crustacean axons. *Biophysical Journal*, 18(1):81–102, April 1977.

- [7] Guillaume Drion, Timothy O’Leary, and Eve Marder. Ion channel degeneracy enables robust and tunable neuronal firing rates. *Proceedings of the National Academy of Sciences*, 112(38):E5361–E5370, September 2015.
- [8] Shaul Druckmann, Yoav Banitt, Albert Gidon, Felix Schürmann, Henry Markram, and Idan Segev. A Novel Multiple Objective Optimization Framework for Constraining Conductance-Based Neuron Models by Experimental Data. *Frontiers in Neuroscience*, 1(1):7–18, October 2007.
- [9] G. Bard Ermentrout and David H. Terman. *Mathematical Foundations of Neuroscience*. Springer Science & Business Media, Berlin, Heidelberg, 2010.
- [10] Urban Forssell and Lennart Ljung. Closed-loop identification revisited. *Automatica*, 35(7):1215–1241, July 1999.
- [11] W. Van Geit, E. De Schutter, and P. Achard. Automated neuron model optimization techniques: a review. *Biological Cybernetics*, 99(4-5):241–251, November 2008.
- [12] Wulfram Gerstner, Werner M. Kistler, Richard Naud, and Liam Paninski. *Neuronal Dynamics: From Single Neurons to Networks and Models of Cognition*. Cambridge University Press, Cambridge, UK, July 2014.
- [13] Joshua H. Goldwyn and Eric Shea-Brown. The What and Where of Adding Channel Noise to the Hodgkin-Huxley Equations. *PLOS Computational Biology*, 7(11):e1002247, November 2011.
- [14] Bertil Hille. *Ionic channels of excitable membranes*. Sinauer Associates, Sunderland, MA, 1984.
- [15] A. L. Hodgkin and A. F. Huxley. A quantitative description of membrane current and its application to conduction and excitation in nerve. *The Journal of Physiology*, 117(4):500–544, August 1952.
- [16] Roger A. Horn and Charles R. Johnson, editors. *Matrix Analysis*. Cambridge University Press, New York, NY, USA, 1985.
- [17] Quentin J. M. Huys, Misha B. Ahrens, and Liam Paninski. Efficient Estimation of Detailed Single-Neuron Models. *Journal of Neurophysiology*, 96(2):872–890, August 2006.
- [18] Eugene M. Izhikevich. *Dynamical Systems in Neuroscience*. MIT Press, Cambridge, MA, 2007.
- [19] James Keener, James Sneyd, S. S. Antman, J. E. Marsden, and L. Sirovich, editors. *Mathematical Physiology*, volume 8/2 of *Interdisciplinary Applied Mathematics*. Springer New York, New York, NY, 2009.
- [20] Hassan K. Khalil. *Nonlinear Systems*. Prentice Hall, Upper Saddle River, NJ, 3 edition, 2002.
- [21] Nathan F. Lepora, Paul G. Overton, and Kevin Gurney. Efficient fitting of conductance-based model neurons from somatic current clamp. *Journal of Computational Neuroscience*, 32(1):1–24, February 2012.
- [22] L. Ljung. Convergence analysis of parametric identification methods. *IEEE Transactions on Automatic Control*, 23(5):770–783, October 1978.
- [23] Lennart Ljung. *System Identification: Theory for the User*. Prentice Hall PTR, Upper Saddle River, NJ, 1999.
- [24] Lennart Ljung. Perspectives on system identification. *Annual Reviews in Control*, 34(1):1–12, April 2010.
- [25] Winfried Lohmiller and Jean-Jacques E. Slotine. On Contraction Analysis for Non-linear Systems. *Automatica*, 34(6):683–696, June 1998.
- [26] I. R. Manchester, M. M. Tobenkin, and J. Wang. Identification of nonlinear systems with stable oscillations. In *2011 50th IEEE Conference on Decision and Control and European Control Conference*, pages 5792–5797, December 2011.
- [27] Robert A. McDougal, Thomas M. Morse, Ted Carnevale, Luis Marengo, Rixin Wang, Michele Migliore, Perry L. Miller, Gordon M. Shepherd, and Michael L. Hines. Twenty years of ModelDB and beyond: building essential modeling tools for the future of neuroscience. *Journal of Computational Neuroscience*, 42(1):1–10, February 2017.
- [28] Lorin S. Milesco, Gustav Akk, and Frederick Sachs. Maximum Likelihood Estimation of Ion Channel Kinetics from Macroscopic Currents. *Biophysical Journal*, 88(4):2494–2515, April 2005.
- [29] Alain Nogaret, C. Daniel Meliza, Daniel Margoliash, and Henry D. I. Abarbanel. Automatic Construction of Predictive Neuron Models through Large Scale Assimilation of Electrophysiological Data. *Scientific Reports*, 6:32749, 2016.
- [30] C. Novara, T. Vincent, K. Hsu, M. Milanese, and K. Poolla. Parametric identification of structured nonlinear systems. *Automatica*, 47(4):711–721, April 2011.
- [31] Johan Paduart, Lieve Lauwers, Jan Swevers, Kris Smolders, Johan Schoukens, and Rik Pintelon. Identification of nonlinear systems using Polynomial Nonlinear State Space models. *Automatica*, 46(4):647–656, April 2010.
- [32] Maarten Schoukens and Koen Tiels. Identification of block-oriented nonlinear systems starting from linear approximations: A survey. *Automatica*, 85:272–292, November 2017.
- [33] Wei Wang and Jean-Jacques E. Slotine. On partial contraction analysis for coupled nonlinear oscillators. *Biological Cybernetics*, 92(1):38–53, December 2004.